SLIP TENDENCY ANALYSIS: IMPLICATIONS ON FAULT REACTIVATION

Barnali Shil

SLIP TENDENCY ANALYSIS: IMPLICATIONS ON FAULT REACTIVATION

Thesis submitted for partial fulfilment

of

Master of Sciences degree

in

Applied Geology

by

Barnali Shil

Under the supervision of

Dr. Tridib K. Mondal

DEPARTMENT OF GEOLOGICAL SCIENCES

JADAVPUR UNIVERSITY, KOLKATA

May 2019

যাদবপুর বিশ্ববিদ্যালয়
কলকাতা-৭০০০৩২, ভারত

JADAVPUR UNIVERSITY
KOLKATA-700032, INDIA

FACULTY OF SCIENCE : DEPARTMENT OF GEOLOGICAL SCIENCES

CERTIFICATE

This is to certify that **Ms. Barnali Shil** (Roll No. 001720402006) of M.Sc. Final Year student of the Department of Geological Sciences, Jadavpur University worked under my guidance and completed the thesis entitled **"SLIP TENDENCY ANALYSIS: IMPLICATIONS ON FAULT REACTIVATION"** for partial fulfillment of the M.Sc. final examination 2019 in Applied Geology of the Faculty of Science, Jadavpur University, Kolkata.

Ms. Shil has fulfilled all the prescribed requirements and this work has not been presented for any degree or diploma elsewhere.

Supervisor
Dr. Tridib Kumar Mondal
Assistant Professor
Department of Geological Sciences
Jadavpur University

Date: 31.5.19

Dr. Tridib Kumar Mondal
Assistant Professor
Department of Geological Sciences
Jadavpur University

31.5.19

Head
Department of Geological Sciences

Date:

Head
Department of Geological Sciences
Jadavpur University
Kolkata-700032

দূরভাষ : ২৪১৪-৬৬৬৬/প্রসারণ : ২২৬৮
Website : www.jadavpur.edu
E-mail : hod_geological@jdvu.ac.in
Phone : 2414 6666/Extn. 2268

Acknowledgement

I would like to thank my supervisor, Dr. Tridib K. Mondal of Department of Geological Sciences, Jadavpur University for his constant support, ideas, encouragement, and patience.

I am very much grateful to Head of the Department, Department of Geological Sciences, Jadavpur University.

I am also thankful to Shreashi Bhowmick for her assistance and helpful discussions during the course of my dissertation. I am thankful to my classmates Arka Pratim and Subhadip for possible help during the work.

I am thankful my family for their love and sincere care for all the time.

Barnali Shil
31.5.2019
Barnali Shil

Abstract

In this study, data from mesoscopic-scale brittle structures (faults) are used to decipher slip tendency analysis and relate it to regional-scale kinematics in granite (Mulgund, West Dharwar Craton, southern India) and it is done using Win Tensor software and it has been found that most of the vulnerable planes are oriented parallel to the compressive direction of D3 deformation.

Key words: Slip tendency, Faults, Win Tensor, Dharwar, India

CONTENTS

LIST OF FIGURES

LIST OF TABLES

CHAPTER 1

Introduction

1.1 General

Fractures and faults are the most common products of brittle deformation. Heterogeneous fault data can be used for fault slip analysis which is an important technique to study the state of stress for a given fault population. As we know that, slip on a plane occurs in the direction of the maximum resolved shear stress (Bott, 1959), we can use the fault slip data for slip tendency analysis which measures how much a plane is likely to slip. Slip tendency analysis is very useful to identify the areas that are highly susceptible to reactivate and therefore prone to earthquakes.

Slip tendency (Ts) is the dimensionless ratio of maximum resolved shear stress to normal stress acting on a surface and is therefore a function of the orientation of the surface of interest and the form of the stress tensor (Morris et al., 1996). Slip tendency

analysis provides useful insights into the distribution of past slip on faults and fractures and the ability to predict behavior of these structures (Morris et al.,1996; Lisle and Srivastava, 2004; Streit and Hillis, 2004; Collettini and Trippetta, 2007). Analysis of slip tendency is predicated on:

(1) Calculation of the state of normal and shear stress for a fault or fracture of any orientation within a stress tensor (e.g., Ramsay, 1967; Ramsay and Lisle, 2000).

(2) The assumption that the resolved shear and normal stresses on a surface are strong predictors of both the likelihood and direction of slip (assumed to be equivalent to the direction of the maximum resolved shear stress) on that surface (Wallace, 1951; Bott, 1959; Lisle and Srivastava, 2004). Although slip tendency is not a direct measure of slip on surfaces, it represents the potential for slip in an applied stress

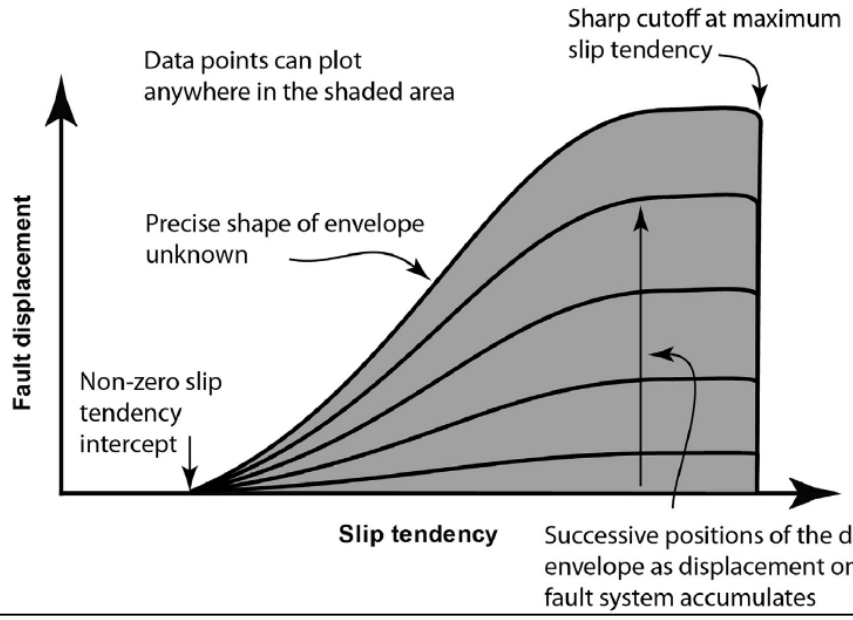

Fig1.1: Conceptual form of the relationship between slip tendency and observed (cumulative) fault displacement. Data from measured fault surfaces could fall anywhere within the shaded area.

state. Patterns of slip tendency are sensitive to the stress ratio ($\Phi=\frac{\sigma 2-\sigma 3}{\sigma 1-\sigma 3}$, Angelier, 1975; Morris et al., 1996; Morris and Ferrill, 2009), and a technique exists that uses this

property to invert stress states using slip tendency analyses without reference to slip directions (McFarland et al., 2012).

1.2 Objectives

The primary objectives of this study are follows:

i) Slip tendency analysis of Mulgund granite, Chitradurga(WDC).

ii) Using slip tendency to find the relation between fault reactivation and regional tectonics.

1.3 Methodology

As highlighted in the section 1.1, the granite replete with faults and fractures in various orientations. To perform slip tendency analysis and obtain the figures, Win Tensor (Delvaux and Sperner,2003) was used.

1.4 Layout of the thesis

The following chapters of this thesis comprise a detailed presentation of data and inferences that help to establish the relationship between regional deformation and brittle structure development in Mulgund granite of the Chitradurga region using the above-mentioned methods and techniques. ***Chapter 2*** consists of a brief description of the regional geological setting of the study area and field structural data and microstructural observations from Mulgund granite. Methology used for this analysis have been discussed in ***Chapter 3***. Fault-slip analysis and related inferences comprise ***Chapter 4***. ***Chapter 5*** comprises conclusions based on the results/inferences from the used methodology.

CHAPTER 2

Regional Geology of the Study area

2.1 Introduction

The Mulgund Granite is located in the western part of the Gadag Schist Belt in the Dharwar craton (southern India; Fig. 2.1). The latter is known to have formed by the accretion of the East Dharwar Craton and West Dharwar Craton at 2.75–2.51 Ga. The zone of accretion is marked by a shear zone, which is referred to as the Chitradurga Boundary Fault, or an easterly dipping thrust (e.g. Naqvi & Rogers 1987; Chadwick *et al.* 2003; Meert *et al.* 2010).

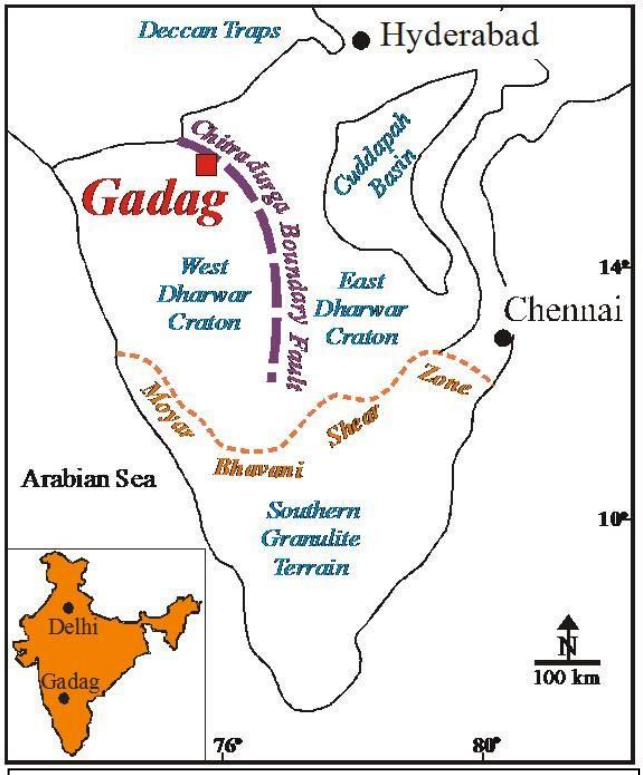

Fig 2.1: Gadag Region (Southern India), after Sarma et al., 2012.

The eastern part of the West Dharwar Craton comprises the Chitradurga Schist Belt. The northernmost part of the schist belt in the vicinity of Gadag is commonly referred to as the Gadag Schist Belt.

2.2 Regional Geology

The Indian shield is consisting of Precambrian metamorphic terrains and mobile belts that comprises low to high-grade crystalline rocks. These Precambrian terrains consist of continental crust and are known as cratons. The Indian shield comprises five major cratons (Dharwar, Bastar, Singhbhum, Bundelkhand and Aravalli) and three mobile belts (Eastern Ghats, Pandyan, and Satpura). These cratons are mainly Archean in age where as the mobile belts are of Proterozoic age. The southern Indian shield consists of two major units- Dharwar craton in the north and Southern Granulite Terrain (SGT) in the south. The Dharwar province exhibits granite-greenstone terrain mainly characterized by several NW-SE to NNW-SSE trending schistose rocks. The SGT is mainly characterized by charnockites, mafic granulites and khondalites which are intersected by several shear zones. Gneisses and supracrustal rocks of amphobolite facies are abundant along with granulite facies rocks. The radiometric dates obtained from SGT show the ages mostly vary between 3000 to 2000 Ma. Dharwar craton (3200 to 3400 Ma) is one of the oldest craton in Indian shield. It broadly comprises three major units - (1) Archean tonalite - trondhjemite - granodiorite (TTG) commonly known as Peninsular Gneissic Complex (PGC); (2) two generations of Archean Greenstone belts (‘schist belt’) represented by Sargur Group and Dharwar Supergroup rocks and (3) late Archean granitoids with or without mantle affiliation. According to Rogers (1986), the Dharwar craton is further divided in two tectonic blocks - Western Dharwar craton (WDC) and Eastern Dharwar

craton (EDC), and the entire Dharwar craton is considered to have formed by the accretion of WDC and EDC at 2510-2750 Ma. The zone of accretion is marked by a shear zone, which is variously referred to as the Chitradurga shear zone. The Closepet granite that lies to the east of the Chitradugra shear zone is the western margin of EDC. The contact between WDC and EDC is not sharp and there is a transition zone between Chitradurga shear zone and Closepet granite. The major difference between WDC and EDC are presented in the Table 2.1.

Western Dharwar Craton (WDC)	Eastern Dharwar Craton (EDC)
1. Dharwar schist belts - large with volcanic, subordinate sediments	1. Dharwar green stone belts -narrow, with dominant pillowed basalts
2. Peninsular Gneiss (>3000 Ma) basement having angular unconformity with the Dharwar. Basement gneiss inliers within schist belt	2. Dharwar batholoth (2500 - 2700 Ma) intusive on all sides. Diapiric gneiss domes are common
3. Three fold succession of: (i) Basalt - arenite-BIF, (ii) Shelf facies at the margin and homotaxial pillowed basalt-BIF in deeper waters, (iii) Greywackes-BIF-volcanics	3. Three folds succession of: (i) Rare shelf sediments disrupted into screens at the belt margins, (ii) Pillowed volcanic, greywackes BIF, (iii) Felsic volcanic , volcanogenic conglomerate ('Champion Gneiss')
4. Older sequence (Sargur Group) as narrow belts and enclaves, abundant in the south	4. Older sequence (Warangal group) mostly as enclaves in the north east; and Salem Group (?) in the south
5. Intermediate pressure (kyanite - sillimanite type) metamorphism	5. Low pressure (andalusite -sillimanite type) metamorphism

Table. 2.1 Difference between Western Dharwar craton (WDC) and Eastern Dharwar craton (EDC) (after Ramakrishnan, 1994; Ramakrishnan and Vidyanandhan, 2010).

The EDC is considered to have formed with island arc accretion to an older (>3500 Ma) solid WDC through transpression. The general stratigraphy of the WDC and EDC is presented in Table 2.2.

The WDC occupies major portions of Peninsular Gneisses and it exhibits various Younger granites (~ 2600 Ma) are mainly exposed in the Chitradurga,

Age	Western Dharwar Craton (WDC)	Eastern Dharwar Craton (EDC)
2500-2600 Ma	Younger granite (Chitradurga, Arsikere) Charnockite	Younger granite/ Gneiss (closepet and equivalents) Charnockite
2600-2800 Ma	Chitradurga Group Dharwar Supergroup Bababudan Group	Kolar Group Yashwantanagar Formation
	---------- unconformity ----------	
~3000 Ma	Peninsular Gneiss	Enclaves older gneiss
3100-3300 Ma	Sargur Group	(?) Warangal Group (?) Salem Group
3300-3400 Ma	Gorur Gneiss	Putative Basement

Table 2.2: Simplified stratigraphy of EDC and WDC (After Swami Nath and Ramkrishnan,1981).

Hosadurga, Arsikere and Banavara region are considered as isolated plutons. These younger granites are considered to have formed due to the crustal reworking. The regional stratigraphy of WDC is presented in Table 2.3. The WDC is significantly different from EDC

in terms of nature and abundance of greenstones as well as the age of surrounding basement rocks. The Archaean TTG is found throughout the WDC and is dated to be 3300 - 3400 Ma. Three generations of volcano-sedimentary greenstone sequences are recorded in the WDC: the 3100 - 3300 Ma Sargur Group, the 2600 - 2900 Ma Dharwar Supergroup, and the 2500 - 2600 Ma calc-alkaline to high potassic granitoids. The regional metamorphic grade of WDC increases from greenschist facies in north to granulite facies in south.

Dharwar Supergroup:The Dharwar Supergroup of WDC is divided into two groups: lower Bababudan Group and upper Chitradurga Group. These are exposed in two lower Bababudan Group and upper Chitradurga Group. These are exposed in two

<table>
<tr><td colspan="5">Proterozoic mafic dykes
Charnokites (2500 - 2600 Ma)
Younger granites (2600 Ma)</td></tr>
<tr><td rowspan="2">Dharwar Supergroup (2800 - 2600 Ma)</td><td rowspan="2">Chitradurga Group</td><td>Ranibennur Subgroup</td><td colspan="3">Greywackes with BIF, polymict conglomerate, volcanic (Maradihalli, Bellara, Medur)</td></tr>
<tr><td>Vanivilas Subgroup</td><td>Polymict conglomerates, cross-bedded quartzite, pelites, stromatolitic carbonates, biogenic cherts, BIF and Mn formation</td><td>Ingaldhal Volcanics</td><td>Tholeiitic basal-rhyolite suit (Tekalvatti, Jagar)</td></tr>
<tr><td colspan="2">Bababudan Group</td><td colspan="3">BIF and Carboneceous phyllites
Basalt-dacite suit (Locally pillowed) with minor ultramafics
Alternatnations of amygdular basalt, cross-bedded quartzites, pelites, minor BIF
Basal Quartz pebble conglomerates</td></tr>
<tr><td colspan="5">----------Fundamental Unconformity----------</td></tr>
<tr><td colspan="5">Peninsular Gneiss (ca. 3000 Ma)</td></tr>
<tr><td colspan="2">Sargur Group (>3000Ma)</td><td colspan="3">Ultramafic-mafic intrusive complexes (Holenatasipur, Nuggihalli)
Surpentinised komatiites, komatiitic and tholeiitic amphibolites, cherts, BIF
Garnet-biotite schist (with kyanite, sillimanite and staurolite)
Local marbles and calc silicates
Fuchsite quartzite with chromite and barites layer</td></tr>
<tr><td colspan="5">(?) Gorur Gneiss (3300 Ma)</td></tr>
</table>

Table 2.3: Simplified stratigraphy of after Swami Nath and Ramkrishnan, 1981.

large schist belts commonly referred as superbelts viz., (1) Bababudan-Western Ghats-Shimoga and (2) Chitradurga - Gadag.. The comprehensive stratigraphic suscession of Dharwar Supergroup are presented in Table 2.3.

Chitradurga- Gadag Superbelts:

Chitradurga-Gadag superbelt is a linear NNW-SSE trending belt, which is about 40km wide in the middle. The northern most part of the schist belt is known as Gadag schist belt. The schist belt represents the thick volcano-sedimentary suite. The dominant rock types of the Chitradurga Schist belt include metabasalt and metagreywacke-argillite sequences interspersed with bands of quartzite, polymict conglomerate and BIF . Anticlinal structure flanked by synclines on either side of the schist belt is observed, near Chitradurga. The Chitradurga Group is commonly divided into two sub-groups: the lower Vanivilas and upper Ranibennur Subgroups (See table 2.3). The Vanivilas Subgroup is conformably overlained by Ranibennur Subgroup. The metavolcanics within the Chitradurga Schist belt are extensively pillowed and show variolitic and agglomeratic structures. The basic volcanics consist of tholeiitic basalt that is metamorphosed in greenschist facies to amphibolites facies. The metabasalts are dated by Sm-Nd method to be 2700 Ma, which corresponds to the age of basaltic eruption. The Chitradurga Schist belt show a series of variably plunging synclines and anticlines with steep NNW-SSE trending axial planes. The major structure is Chitradurga anticline, upright fold with undulating axial plane and near vertical plunge. The anticline is flanked on either side by synclines and interpreted as a second generation folding. A major sinistral shear zone marks the eastern boundary of the schist belt. This prominent NW-SE to NNW-SSE trending shear zone marks the transitional boundary between WDC and EDC.

Younger Granites:

Younger Granites (2500 – 2600 Ma) occur as isolated discrete intrusion cutting across the foliations and banding of Peninsular Gneiss/TTG. Some of them intrude the schist belt also, like the Chitradurga granite. These are considered to have formed due to reworking of older crust. Various younger granites that are exposed near Chitradurga region are described below.

Chitradurga Granite: The Chitradurga granite is a narrow curvilinear pluton extending from Chitradurga to Rangayandurga for a distance of 60 km. Its western contact is with Gneissic complex except for the northern tip and its eastern contact is with the schist belt. In northern part, this granite is sheared along its eastern margin. It is typically massive, nonfoliated, occasionally crudely foliated, coarse grained and equigranular with composition varying from granite to granodiorite (Chakrabarti et al., 2006). It is intruded both into gneissic complex and the schist belt.

Hosadurga Granite: It is a curvilinear spindle shaped granitic body intrusive into the Peninsular Gneiss between Holalkere in the north and Hundirakere in the south. It has the same general NNW-SSE tectonic trend as the western margin of Chitradurga Schist belt. It is possibly emplaced along the core of the antiform of Chiknayakanhalli.

Jampalnaikankote Granite: This is a large oval body of granite exposed in the eastern border of Chitradurga Schist belt around Jampalnaikankote, Sondekere, Vaddikere villages. This composite granite body shows variation in composition from diorite through quartz diorite, granodiorite to granite. The granite is essentially coarse grained with crude foliation at places and consists of microcline, albite, hornblend, biotite and garnet (Chakrabarti et al., 2006).

2.3 Geology of the study area

As shown in Figure 1b, the Mulgund Granite, which is the focus of the present investigation, is located to the west of the metabasalts. U–Pb geochronology of the granite indicates an age of *c*. 2.5 Ga (Sarma *et al*. 2011). The granite occupies an area of *c*. 300 km2, and lacks a well-developed mesoscopic foliation in most places (Fig. 2a). The anisotropy in such visibly isotropic granites is commonly

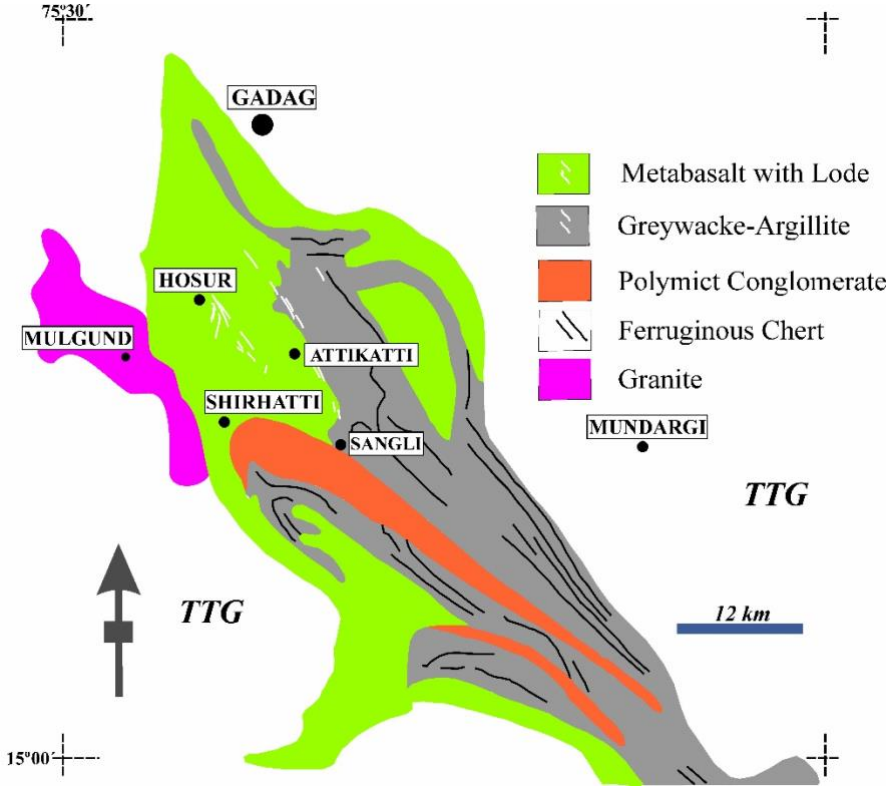

Fig 2.2: Lithology of the studied area, after Modified after Curtis and Radhakrishna, 1993.

recognized from anisotropy of magnetic susceptibility (AMS) studies (e.g. Bouchez 1997). Based on AMS analysis Mondal & Mamtani (2014) have shown that the magnetic foliation in the granite has a mean orientation of 343°/54°E, and the magnetic lineation is doubly plunging (to the NW and SE). This magnetic fabric is similar to that recorded in the metabasalts (Mondal & Mamtani 2013, 2014). It may be noted that the mean strike of the magnetic foliation in rocks of the Gadag region (granite and

metabasalt) is 339°. Petrographic studies reveal the presence of biotite, quartz, K-feldspar, plagioclase and magnetite. Large grains of zoned feldspar, which is a remnant of the original igneous texture, are commonly preserved. Textures indicating superimposition of low-*T* over high-*T* solidstate deformation fabrics are common. The presence of a chessboard pattern in quartz indicates that the solid-state deformation in the granite took place at high temperature (>650°C; Kruhl 1996). This texture also implies that the granite was emplaced syntectonically (Paterson *et al*. 1989; McCaffrey *et al*. 1999; Mamtani & Greiling 2005), and that crystal plasticity began at temperatures close to the solidus (Mainprice *et al*. 1986). Medium-*T* solid-state deformation is inferred from the presence of myrmekite and deformation twins in feldspar (Vernon 2004; Passchier & Trouw 2005). Furthermore, quartz grains show dynamic recrystallization by bulging, which indicates low-*T* solid-state deformation (280–400°C; Stipp *et al*. 2002; also see Sen & Mamtani 2006; Mamtani & Greiling 2010). All the above-described textures indicate that the Mulgund Granite is deformed and developed deformation textures as the granite cooled and crystallized. It has been concluded that the Mulgund Granite was emplaced syntectonically with regional D1–D2 deformation that occurred under regional NE–SW compression and resulted in NW–SE magnetic foliation. Subsequently, the granite was subjected to D3 deformation under NW–SE compression, which resulted in the doubly plunging attitude of magnetic lineation; this is similar to dome–basin interference on account of superimposed deformation (Mondal & Mamtani 2014). Evidence of strain localization is recorded at the contact between the TTG and the Mulgund Granite. The gneissosity (foliation) in the TTG is NW–SE striking (*c*. 335°) away from the contact, and tends to become parallel to the *c*. 305°-oriented contact between the granite and the gneiss. This sinistral sense of shear is also inferred from the S–C fabric that has developed in the mylonitized

gneiss at the contact. Evidence of sinistral strike slip movement is also recorded in the granite at the same contact. However, because the slickenfibres have an oblique orientation on the fault plane, the faults are categorized as oblique-slip normal faults. Based on the above description, the Mulgund Granite can be considered as an ideal example in which structures developed under different conditions are preserved; namely, from high temperature to low-temperature solid-state deformation ductile structures , as well as brittle deformation structures.

2.4 Lithology

Ultramafic rocks and Peninsular Gneiss

The ultramafics of this region are mainly enclaves which are present within the gneissic rocks. Compositionally these are talc-actinolite and talc-tremolite schist. Peninsular gneiss, basement of the schist belt belongs to Older Peninsular Gneissic complex. The gneisses show mixed assemblage of granitic gneisses, migmatite and biotite and hornblend gneisses. The rocks are greyish white in color and and show well developed gneissosity, defined by alternating layers of felsic and mafic minerals. The gneisses are tonalitic, trondhjemitic to granodioritic in composition (2900-3000 Ma). Banded migmatitic gneisses and quartzofeldspathetic gneisses are commonly found in this region.

Metavolcanic

Chitradurga region represents the volcano-sedimentary rocks which have accumulated in the deep marine environment in a progressively sinking basin (Ramakrishnan and Vaidyanadhan, 2010). The volcanic rocks of the Chitradurga region are metamorphosed to lower greenschist to amphibolite facies. The massive meta-

basalts are fine grained, dark grey to greenish grey in color and almost aphanitic. The metabasalts are massive in nature and show pillowed structures. However, the foliated metabasalts are also observed in various places. Several radial cracks on pillow head are reported (Chakrabarti et al., 2006). Columnar jointing has been observed in several places. The overall geochemistry indicates that the volcanic pile is composed of tholeiites, basaltic andesites, andesites and rhyo-dacites with calc-alkaline affinity. Agglomerate, tuffs and cherts are very common. The associated iron formation is of sulfide facies.

Argillite, Phyllite and Greywacke

The argillite and schist are very common metasedimentary rocks in this region. The greywacke types of sediments represent a monotonous succession of alternating bands of greywacke and argillite. The greywacke varies in composition from quartz wacke to lithic wacke and contains flute casts, sole marks etc. The greywacke represent the deep marine facies. In all possibility these greywackes represent post-orogenic sediments of the region. The greywacke phyllite suit is frequently interbedded with BIF, volcanics, pyroclastics, and polymictic conglomerate and probably represents an offshore deposit.

Banded Iron Formation

Banded iron formations represent a distinct type of sedimentary unit common in this region. The formations are characteristically banded with alternating bands of chert and iron ore. They are frequently seen in association with volcanic rocks and source of much of the iron and silica appears to be volcanogenic (Ramakrishnan and Vaidyanadhan, 2010). Clastic sediments are absent. Reddish ferruginous shales and phyllites are common associates.

Younger Granites

The younger granite (Fig. 3.3a) consists of multiple intrusions emplaced within the Peninsular Gneissic complex. Coarse grained porphyritic potassic granite with large sized porphyroblusts of grey or pink colored microcline is the most characteristics feature of this granite. The granites are grey in color, characteristics feature of this granite (Fig. 3.3b). The granites are grey in color, medium to coarse grained, containing quartz, feldspar, biotite and hornblend as essential minerals and magnetite as accessories. The granite is considered to be a diapiric intrusion and show enclaves of gneiss and/or microgranitoids at few places which supports the early workers sugession (Jayananda et al., 2006; Sarma et al., 2011) that granite was formed by reworking of crustal rocks. The present investigation is aimed at analyzing the fabric in younger granites which is visibly isotropic in nature.

2.5 Field structures

According to previous researchers such as Chakrabarti et al., 2006, the structural pattern of Chitradurga Schist belt is similar to Gadag Schist belt. The structural investigation of the adjacent meta-sedimentary rocks of the region revealed that the area has undergone three phases of deformation: D1, D2, D3 (Chadwick et al., 1989; Jayananda et al., 2006). Regionally D1/D2 are coaxial with NW striking axial plane. The mesoscopic field structures are mainly observed in the BIF, phyllite, argillite, greywacke associated to this region. But the granites are visibly isotropic and show lack of well-developed foliation.

2.5.1 Structures in supracrustal rocks

Three generation of folds are recognized in the Chitradurga region. F1 folds are reported as tight, isoclinal fold whereas F2 folds are open to tight and upright and F3 folds are regionally open with NE-SW striking vertical axial plane. According to Sengupta and Roy (2012), NE-SW directed shortening was responsible for the development of the NW-SE oriented structural elements (F1/F2 folds) in the Chitradurga Schist belt. Whereas F3 fold was an account of NW-SE shortening which superimpose the earlier structures, forming culmination and depression in the region (Chakrabarti et al., 2006).Thus, the above studies indicate that the structural evolution of the Chitradurga Schist belt is controlled by early NE-SW compression followed by late NW-SE compression.

2.5.2 Structures in Mulgund granite

The granite in the study area is massive and don't show any mesoscopic field foliation. Petrographic study inferred the presence of minerals like quartz, K-feldspar, plagioclase and biotite. In common large grains of zoned k-feldspar are present which indicate the remnant of original igneous texture (Fig. 2.3a). Chess-board pattern of quartz is present in granite which is characterized by square sub-grains with boundaries parallel to both prism and basal planes (Fig.2.3b) (Khuhl, 1996). This texture indicate that crystal plasticity begins at temperature close to solidus (Mainprice et al., 1986) and implies high temperature solid-state deformation at T>650ºC (Khuhl 1996). Some of the quartz grains also show dynamic recrystallization by subgrain rotation (Fig. 2.3c), which is a characteristics of solid-state deformation at medium temperature of 400-500ºC (Stipp et al., 2002; Passchier and Trouw, 2005). Myrmekite and deformation twins in feldspar (Fig. 2.3d) and other textures that imply solid-state deformation at medium to high temperature (Vernon, 2004; Passcher and Trouw, 2005; Mamtani and Greiling, 2010).

Bulging (dynamically recrystallised) quartz grains are also observed, which develop at low temperature condition (280-400ºC; Stipp et al., 2002). It is evident from the above texture that Chitradurga granite is deformed and it developed deformation texture as

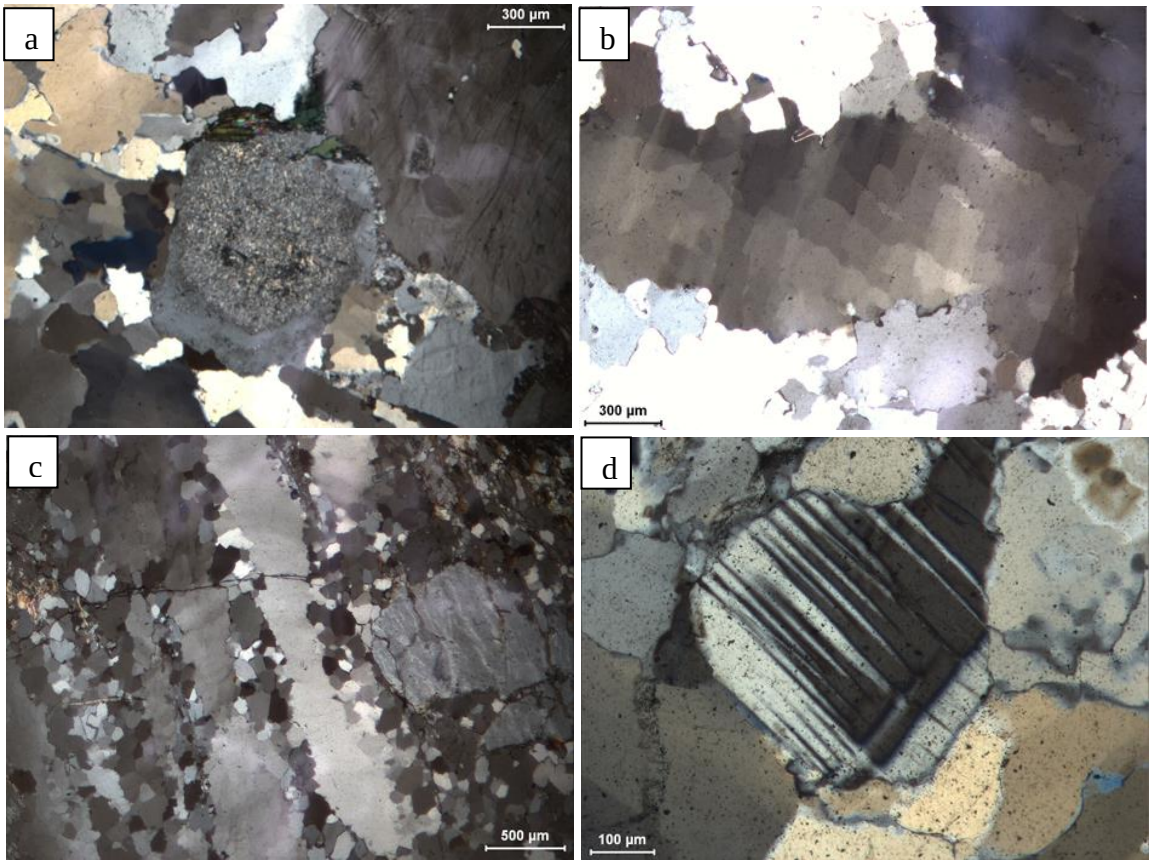

Fig.2.3 Texture in Younger granite (a) Zoned feldspar (altered) indicating remnant of original igneous texture in granite (b) Chessboard pattern in quartz indicating high-T solid-state deformation (c) Quartz grain showing sub-grain rotation crystallization (d) Deformation twin in feldspar, after Mondal,2017.

the granite cooled from high to low temperature (also see Sen and Mamtani, 2006; Mamtani and Greiling, 2010.

CHAPTER 3

Methodology

3.1 Introduction

Slip tendency analysis is based on the premise that the resolved shear and normal stresses on a surface are strong predictors of both the likelihood and direction of slip on that surface (Morris etal., 1996). The method has been used successfully to characterize fault slip (Streit and Hillis,2004) and fault slip directions (Lisle and Srivastava,2004; Collettini and Trippetta,2007). Fractures in high- slip-tendency orientations are, in many cases, better flow conduits than fractures in low-slip-tendency orientations (Bartonetal., 1995; Morris et al., 1996; Ferrill et al.1999; Sibson, 2000). The effect of stress anisotropy is greatest when the effective stress conditions on a fault or fracture

approach those required for slip: the so-called critical stress (Stocketal, 1985; Wiprut andZoback,2002; Zhang et al.,2007). Thus, preferential fluid flow through fault and fracture pathways is more pronounced the greater the differential stress and the greater the area off sand fractures experiencing high slip tendency (Zobacketal.,1996; Morris et al.,1996; Ferrilletal.,1999; Takatoshi and Kazuo,2003). Formally, the slip tendency (Ts) of a surface is defined as the ratio of shear stress (τ) to normal stress (σ_n) on that surface (Morris etal.,1996):

$$Ts=\tau/\sigma_n.$$

The slip tendency is only a function of the stress tensor and the orientation of the surface. Whether or not slip occurs will depend on the coefficient of static friction (e.g., Byerlee, 1978). For cohesion less surface, slip occurs when the slip tendency exceeds the coefficient of static friction. In addition, the magnitude of the effective intermediate principal stress (σ_2) relative to the effective maximum and minimum principal stresses has a profound influence on the slip tendency pattern (Morris and Ferrill,2009).

3.2 Methodology

Over time, and under stable stress conditions, we would expect that fault orientations experiencing persistently high slip tendency would accumulate more displacement than those with lower slip tendencies because they are likely to slip more frequently and with larger increments of slip, and that some orientations would not be represented at all. Conceptually, there would be a positive correlation between slip tendency and cumulative fault slip, but with a non-zero slip tendency intercept. An individual slip surface that has a high slip tendency orientation will not necessarily have accumulated a large amount of displacement because it may have either been in the stress shadow of a larger slip surface or only have formed late in the deformation history and not

experienced many slip increments. Because new slip surfaces may form at any time, surfaces with high slip tendencies may be represented by multiple displacement values from high to low, but surfaces with lower slip tendencies only will exhibit lower values of displacement. Hence, the distribution of points in displacement versus slip tendency parameter space should be a cloud with variable values of displacement for a given slip tendency, but with decreasing displacement range with decreasing slip tendency. There is likely to be a sharp cutoff of the distribution at the slip tendency value that corresponds to the maximum strength of the rock under the deformation conditions in which the fault population formed. An evolving fault system would exhibit differing data envelopes as displacement accumulates.

3.3 Slip Tendency analysis

In paleostress analyses, the best-fitting stress tensor for a population of faults and striations is computed by minimizing the mean deviation angle between the data set of measured striations and the theoretically calculated striations. The routine is an inversion of a method to obtain from a state of stress the sense of movement on a fracture plane with given orientation (Bott, 1959). Several computer routines for the inversion procedure have been developed during the last fifteen years. Most routines are based on a method of paleostress analysis described in Angelier et al. (1982). Other programs use a simplified inversion technique proposed by Michael (1984). A disadvantage of most programs is that the user has little control on the process of fitting the theoretical tensor to the data. This disadvantage has been eliminated in a program recently developed by Delvaux (2003), named Win Tensor which we have used in the presented analysis. All programs calculate relative magnitudes for the principal stress axes only, while for absolute magnitudes for the vertical principal stress axes

information on the lithostatic pressure during the tectonic event is needed. Further, limitations and assumptions of the paleostress method are extensively reviewed in Angelier (1994).

The results of the optimization procedure are given by the orientation of the three principal stress axes and some parameters defining the quality of the obtained results. In all cases the results satisfy the relationship. An indication of the shape of the stress ellipsoid is given by the ratio R, which is defined as: $R=\frac{\sigma 2-\sigma 3}{\sigma 1-\sigma 3}$

The quality of the fit of the theoretical tensor to the selected subset is expressed by the slip deviation. This parameter represents the angle of deviation between the theoretical striations and the observed striations of the stress site. The a-angle is the parameter which is optimized during the calculations. Striations that deviate more than 30° were in all cases rejected for the calculation of the tensor axes. These rejected measurements could then afterwards be tested on homogeneity for a second phase of fault movement. For the applied method only monophase data sets can be used. The study area, however, is characterized by a polyphase brittle deformation history. The used program offers an indication for the homogeneity of a subset from the data, by means of the Mean Counting Deviation (Mean CD). This is a statistical method that expresses to what extent the selected fault planes have common extension and compression dihedra (Angelier and Mechler, 1977). With a standard deviation below l0 the data set can reasonably be assumed to be mono phase. A second parameter which gives an indication of the relative quality of the calculated tensors is the tensor accuracy rank which is defined by Delvaux (1994) as:

Tensor Rank= $\frac{N(\frac{N}{No})}{\alpha}$;

Where N being total number of measurements at one site and No is the total number of faults that fitted within one regime.

CHAPTER 4

Results and Discussions

4.1 Introduction

In this present thesis, fault data from Mulgund granite has been analyzed by Slip Tendency analysis method using Win Tensor (Delvaux & Sperner,2003). In this Chapter, the details of the slip tendency analysis results has been discussed.

4.2 Results

In this study 97 fault-slip data (orientation of fault plane and lineation) were collected from Mondal & Mamtani (2014), from a total of 13 sites spread across the Mulgund Granite. It is found that a majority of fault planes are WNW–ESE striking (285°) with a sub-maximum in a NW–SE direction (325°). Most of the fault planes have moderate to steep dips with the mean dip amount being 48°. The pitch of the slickenfibres (lineation) on the fault planes is variable, with a mean of 37°. This indicates that the faults are mainly oblique-slip normal faults.

The data sites has been divided into 4 zones, depending upon similar fault data and spatial spreading. Data from these 4 zones have been analyzed individually.

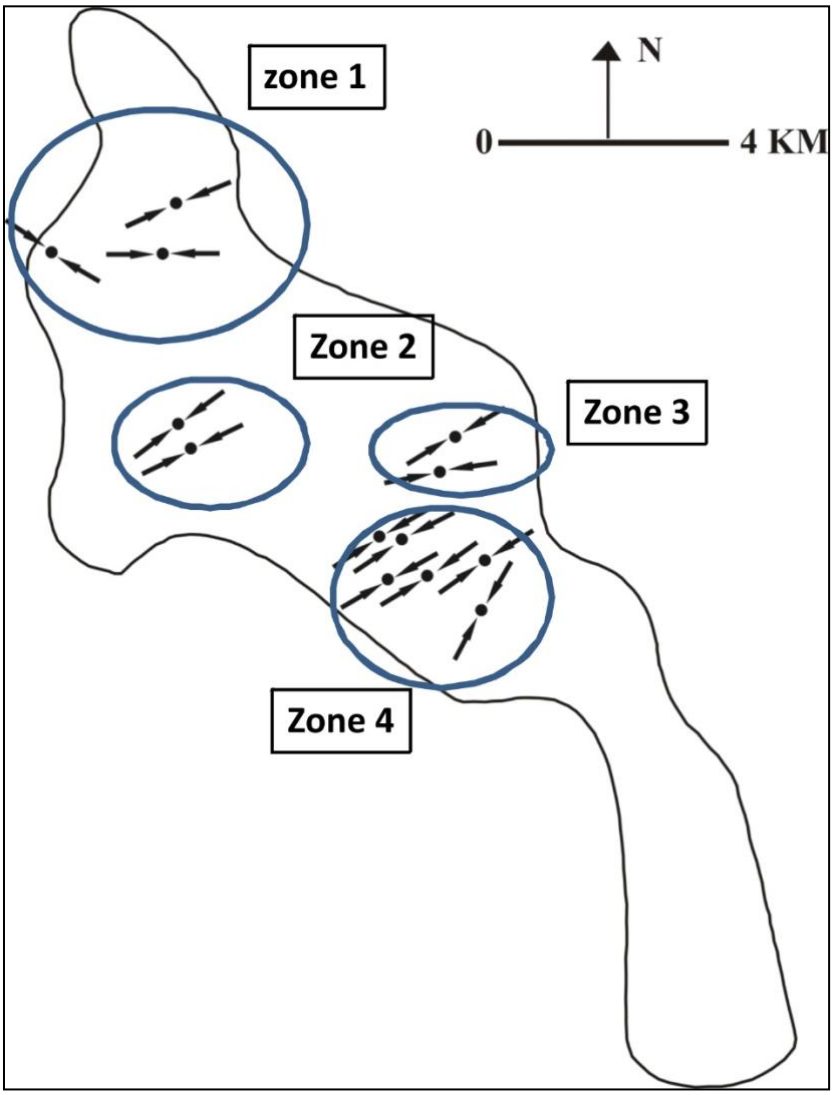

Fig 4.1: Map of Mulgund granite demarcating the zones.

Data from each zone have been put through Win Tensor and Right dihera method has been used for data separation and obtaining Mohr circle figures. The obtained homogeneous data gives us the tensor of that following zone and a map has been prepared using that tensor to give us an overall idea about the tensor distribution over that region.

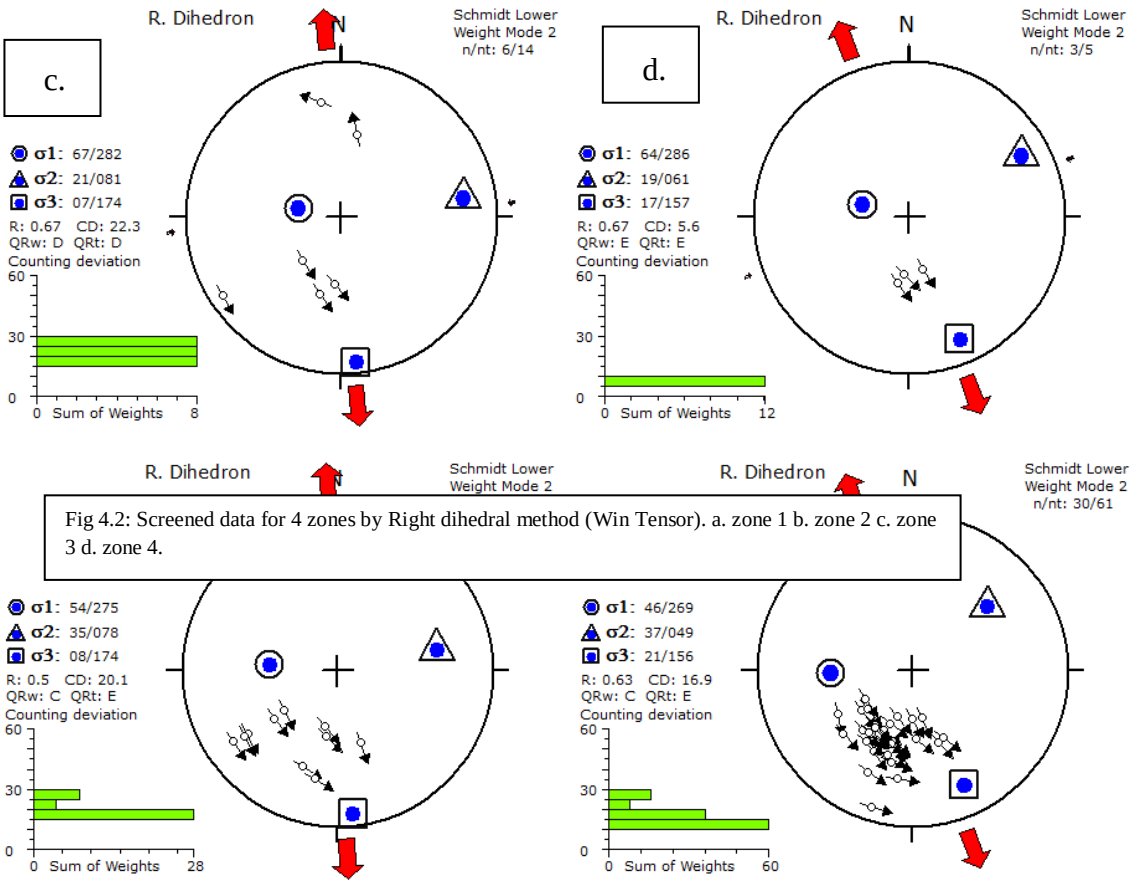

Fig 4.2: Screened data for 4 zones by Right dihedral method (Win Tensor). a. zone 1 b. zone 2 c. zone 3 d. zone 4.

After that 2D rose diagrams were created alongwith the orientations of the planes which are screened already. The planes are demarcated using a color profile to denote the magnitude of slip tendency, dark red color having slip tendency value around 0.8-1 and blue color having value around 0-0.2. These orientations of the planes are compared with the regional D3 deformation and a relation has been found. It has already been established that the direction of the compression direction of D3 deformation in Mulgund granite is ENE-WSW (Mondal & Mamtani,2016).

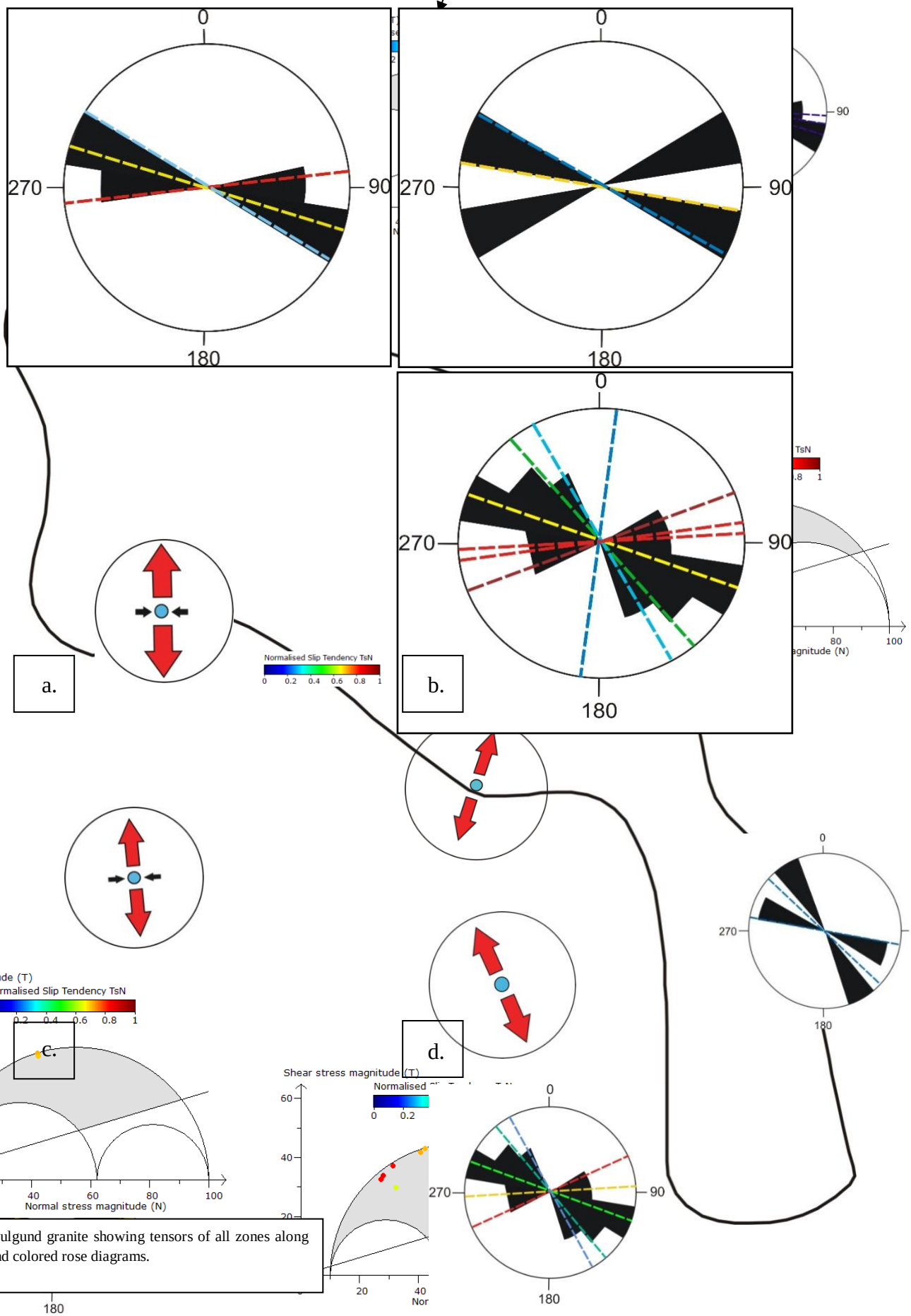

Fig 4.3: Map of Mulgund granite showing tensors of all zones along with Mohr circle and colored rose diagrams.

Fig 4.4: Rose diagrams showing orientations of screened planes. a.Zone 1(inset- slip tendency color coordinated value) b. Zone 2 c. Zone 3 d. Zone 4.

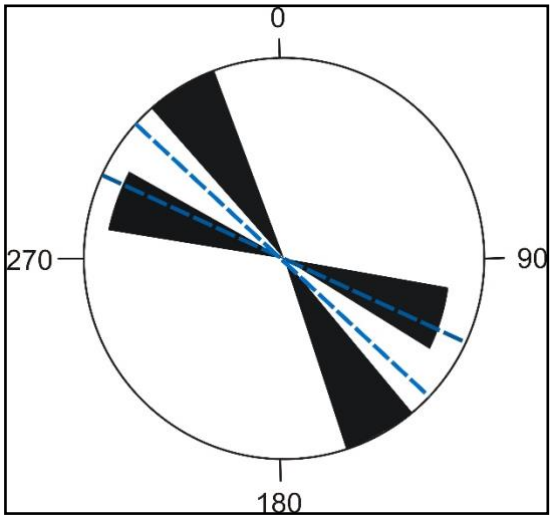

4.3 Discussions

As it has been mentioned earlier that the direction of compression of D3 deformation in Mulgund granite is ENE-WSW direction, we can see in the colored rose diagrams (Fig 4.4) that the planes having higher slip tendency values are oriented parallel to the compressive direction of D3 deformation. And as the planes are oriented at a higher angle to the compression direction of D3 deformation, the value of slip tendency decreases, indicating that those planes are much less susceptible to reactivate if subjected to stress. Slip tendency analysis is an efficient tool to identify weaker planes in a region such like this. With further studies in this topic, we can even generate a slip tendency map of any region given that we know the regional stress tensor.

CHAPTER 5

Conclusions

5.1 Introduction

The objective of this study is to understand slip tendency analysis and apply it to the Mulgund granite(West Dharwar Craton,South India).After using Win Tensor(Delvaux & Sperner,2003) to perform slip tendency analysis, the conclusions are discussed in this chapter, along with scope for future work.

5.2 Conclusions

1. The planes oriented parallel to the compression direction of D3 deformation in Mulgund granite show higher slip tendency value (about 0.8-1) and the planes oriented at a high angle (about 70°-90°) with respect to the compression direction

of D3 deformation show much less value of slip tendency (0.2-0.5). This means that the first mentioned fault planes are much more susceptible to reactivate than the planes oriented in other manner.

2. Heterogeneous dataset can be modified into homogeneous dataset to generate a stress tensor.

3. Win Tensor is an outstanding tool to use for fault slip analysis, especially slip tendency analysis and can generate stress tensor of a given fault population. It can also differentiate fault data generated by different deformations.

5.3 Scope for future work

1. Slip tendency analysis can also be done in different lithologies for generate stress tensor and fine planes prone to failure.

2. Using this method, we can also demarcate earthquake prone areas where fault planes are not prominent or covered by soil, given we know the regional stress tensor model and fault data from neighboring region.

REFERENCES

Angelier, J., 1994. Fault slip analysis and palaeostress construction. In: Hancock, P.L. (Ed.), Continental Deformation. Pergamon Press, London.

Balakrishnan, S., Hanson, G. N., Rajamani, V., 1999. U–Pb ages for zircon and titanite from the Ramagiri area, southern India: evidence for accretionary origin of the Eastern Dharwar Craton during the late Archean. Journal of Geology 107, 69–86.

Blenkinsop, G. T., 2006. Kinematic and dynamic fault slip analyses: implications from the surface rupture of the 1999 Chi–Chi, Taiwan, earthquake. Journal of Structural Geology 28, 1040–1050.

Chadwick, B., Vasudev, V. N., Hegde, G. V., 1999. Magmatism, structure, emplacement and plate tectonic setting of late Archaean Dharwar batholith, south India. Department of Mines and Geology, Government of Karnataka, Geological Studies 316, 67.

Chadwick, B., Vasudev, V. N., Hegde, G. V., 2000. The Dharwar Craton, southern India, interpreted as the result of Late Archaean oblique convergence. Precambrian Research 99, 91–111.

Chadwick, B., Vasudev, V. N., Hedge, G. V., 2003. The Chitradurga schist belt and its adjacent plutonic rocks NW of Tungabhadra, Karnataka: a duplex in the late Archean convergent setting of the Dharwar craton. Journal of the Geological Society of India 61, 611–613.

Chadwick, B., Ramakrishnan, M., Vasudev, V. N., Viswanatha, M. N., 1989. Facies Distributions and Structure of a Dharwar Volcanosedimentary Basin: Evidence for Late Archaean transpression in Southern India? Journal of the Geological Society of London 146, 825–834.

Chadwick, B., Vasudev, V. N., Hedge, G. V., Nutman, A. P., 2007. Structure and SHRIMP U/Pb zircon ages of granites adjacent to the Chitradurga schist belt: implications for Neoarchaean convergence in the Dharwar craton, southern India. Journal of the Geological Society of India 69, 5–24.

Cowie, P. A., Scholz C. H., 1992. Physical explanation for the displacement-length relationship of faults using a post-yield fracture mechanics model, Journal of Structural Geology 14(10), 1133-1148.

Delvaux, D., Barth, A., 2010. African stress pattern from formal inversion of focal mechanism data. Tectonophysics 482, 105–128.

Delvaux, D., Sperner, B., 2003. Stress tensor inversion from fault kinematic indicators and focal mechanism data: the TENSOR program. In: Nieuwland, D. (Ed.), New Insights into Structural Interpretation and Modelling: Geol. Soc. Lond. Special Publication 212, 75–100.

Doblas, M., 1998. Slickenside kinematic indicators, Rock deformation; the Logan volume. Elsevier, Amsterdam, Netherlands 187-197.

Dresen, G., 1991. Stress distribution and the orientation of Riedel shears. Tectonophysics 188, 239–247.

Dupin, J. M., Sassi, W., Angelier, J., 1993. Homogeneous stress hypothesis and actual fault slip: a distinct element analysis. Journal of Structural Geology 15, 1033–1043.

Etchecopar, A., Vasseus, G., Daigniers, M., 1981. An inverse problem in microtectonics for the determination of stress tensor from fault striation analysis. Journal of Structural Geology 3, 51–65

Fleischman, K. H., Nemcok, M., 1991. Paleostress inversion of fault/slip data using the shear stress solution of Means (1989). Tectonophysics 196, 195–202.

Fleuty, M. J., 1974. Slickensides and slickenlines. Geological Magazine 112(3), 319-322.

Jayananda, M., Chardon, D., Peucat, J.-J., Capdevila, R., 2006. 2.61 Ga potassic granites and crustal reworking in the western Dharwar craton, southern India: tectonic, geochronologic and geochemical constraints. Precambrian Research 150, 1–26.

Manikyamba, C., Naqvi, S. M., Subba Rao, D. V., Ram Mohan, M., Khanna, T. C., Rao, T. G., Reddy, G. L. N., 2005. Boninites from the Neoarchaean Gadwal Greenstone belt, Eastern Dharwar Craton, India: implications for Archaean subduction processes. Earth and Planetary Science Letters 230, 65-83.

Manzocchi, T., Walsh, J. J., Nicol, A., 2006. Displacement accumulation from earthquakes on isolated normal faults. Journal of Structural Geology 28, 1685-1693

Marrett, R., Allmendinger, R. W., 1990. Kinematic analysis of fault–slip data. Journal of Structural Geology 12, 973–986.

McFarland, J.M., Morris, A.P., Ferrill, D.A., 2012. Stress inversion using slip tendency. Comput. Geosciences 41, 40-46.

Michael, A. J., 1984. Determination of Stress from Slip Data: Faults and Folds. Journal of Geophysical Research 89, 11517-11526.

Mondal, T.K., Mamtani, M.A. 2016. Palaeostress analysis of normal faults in granite–implications for interpreting Riedel shearing related to regional deformation. Journal of the Geological Society, 173, 216–227.

Morris, A.P., Ferrill, D.A., Henderson, D.B., 1996. Slip tendency and fault reactivation. Geology 24, 275-278.

Nicol, A., Walsh, J. J., Villamor, P., Seebeck, H., Berryman, K. R., 2010, Normal fault interactions, paleoearthquakes and growth in an active rift: Journal of Structural Geology 32 (8), 1101–1113.

Radhakrishna, B., P., Vaidyanadhan, R., 1997. Geology of Karnataka. Geological society of India. Second Edition.

Rajabi, S., Eliassi, M., 2012. Kinematic and Dynamic Analysis of North-Tehran Tectonic Wedge Formed in South Central Alborz, Iran. Journal Geological Society of India, 80, 731-737.

Ramsay, J. G., Lisle, R. J., 2000. The Techniques of Modern Structural Geology. Vol. 3: Applications of Continuum Mechanics in Structural Geology. Academic Press, London.

Rollinson, H. R., Windley, B. F., Ramakrishnan, M., 1981. Contrasting high and intermediate pressures of metamorphism in the Archaean Sargur Schists of southern India. Contributions to Mineralogy and Petrology 76, 420–429.

Sarma, D. S., Fletcher, I. R., Rasmussen, B., McNaughton, N. J., Mohan, M. R., Groves, D. I., 2011. Archean gold mineralization synchronous with late cratonization of the Western Dharwar Craton, India: 2.52 Ga U–Pb ages of hydrothermal monazite and xenotime in gold deposits. Mineralium Deposita 46, 273–288.

Sengupta, S., Roy, A., 2012. Tectonic Amalgamation of Crustal Blocks along Gadag Mandya Shear Zone in Dharwar Craton of Southern India. Journal of the Geological Society of India 80, 75–88.

Twiss, R. J., Unruh, J. R., 1998. Analysis of fault slip inversions; do they constrain stress or strain rate? Journal of Geophysical Research 103 (B6), 12205–12222.

Yamaji, A., 2000. The multiple inverse methods: a new technique to separate stresses from heterogeneous fault-slip data. Journal of Structural Geology 22, 441–452.

Yamaji, A., Sato, K., 2006. Distances for the solutions of stress tensor inversion in relation to misfit angles that accompany the solutions. Geophysics Journal International 167, 933–942.

Yamaji, A., Otsubo, M., Sato, K., 2006. Paleostress analysis using the Hough transform for separating stresses from heterogeneous fault–slip data. Journal of Structural Geology 28, 980–990.

Yin, Z. M., Ranalli, G., 1992. Critical stress difference, fault orientation, and slip direction in anisotropic rocks under non-Andersonian stress system. Journal of Structural Geology 14, 237-244.

Žalohar, J., Vrabec, M., 2007. Paleostress analysis of heterogeneous fault–slip data: the Gauss method. Journal of Structural Geology 29, 1798–1810.